Hindawi Publishing Corporation
Journal of Nanomaterials
Volume 2016, Article ID 3427809, 8 pages
http://dx.doi.org/10.1155/2016/3427809

Research Article

Peroxidase-Like Activity of Ferrihydrite and Hematite Nanoparticles for the Degradation of Methylene Blue

Nicolaza Pariona,[1] M. Herrera-Trejo,[2] J. Oliva,[2] and A. I. Martinez[2]

[1]*Red de Estudios Moleculares Avanzados, Instituto de Ecología, AC 91070, Carretera Antigua a Coatepec 351, El Haya, Xalapa, VER, Mexico*
[2]*Center for Research and Advanced Studies of the National Polytechnic Institute, Cinvestav-Saltillo, 25900 Ramos Arizpe, COAH, Mexico*

Correspondence should be addressed to A. I. Martinez; arturo.martinez@cinvestav.edu.mx

Received 7 August 2016; Revised 24 August 2016; Accepted 4 September 2016

Academic Editor: Jean M. Greneche

The peroxidase-like catalytic properties of 2-line ferrihydrite (2LFh) and hematite nanoparticles (NPs) for the degradation of methylene blue (MB) were studied. It is highlighted that the hematite NPs were prepared from the transformation of the metastable 2LFh NPs. It was found that the 2LFh NPs exhibited poor crystallinity with an average size of 5 nm, while the hematite NPs exhibited high crystallinity with an average size of *ca*. 100 nm. It was found that the total degradation of MB occurred for hematite NPs, while only a maximum degradation of 69% was possible for the 2LFh NPs. The Michaelis–Menten parameters indicated that the hematite NPs present higher catalytic activity than the 2LFh NPs at basic pH. It was found that the ordered surface of the hematite NPs has a stronger effect for the degradation of MB than its low surface area. It was concluded that the crystal planes of the hematite NPs affect the catalytic process more significantly than the high surface area of 2LFh NPs.

1. Introduction

Peroxidases are a group of enzymes found in bacteria, fungi, plants, and animals which in presence of hydrogen peroxide (H_2O_2) catalyze the oxidation of organic and inorganic compounds [1]. These enzymes can act as antioxidants and as defense against pathogen agents [2, 3]. They also have potential applications in different fields such as biomedicine, for the construction of diagnostic kits and enzyme immunoassays [2, 4]. Additionally, in environmental science, peroxidases are used for the degradation of organic contaminants [5]. Particularly, natural peroxidases such as the horseradish peroxidase oxidize various organic compounds including phenol [6]. Peroxidases contain Fe^{3+} or Fe^{2+} ions in their active sites, which catalyze the oxidation of organic substances in presence of H_2O_2. Such catalytic process involves Fenton reactions which generate hydroxyl radicals (•OH) [7]; these radicals are useful for the degradation of organic compounds in residual water. However, the application of these enzymes in wastewater treatment is limited due to their poor stability and elevated cost [4, 8]. Due to the many disadvantages for the applications of natural peroxidases in wastewater treatment, the exploration of artificial peroxidase-like compounds has been an active topic of research [9–11].

Iron oxide nanoparticles (NPs) have attracted great attention because their outstanding catalytic activity is similar to that for peroxidases [12]. The iron oxide NPs show other advantages such as stability at different pH, low cost, and high abundance [2]. Peroxidase-like activity has been explored in NPs of different iron oxides polymorphs such as ferrihydrite [13], hematite [13], magnetite [14, 15], maghemite [16], and goethite [17]. In general, it was found that peroxidase-like activity of iron oxide NPs may be affected by the size, shape, and concentration of the NPs [12, 18–20]. Additionally, the crystal structure of the iron oxide NPs and their behavior in aqueous media may affect the catalytic activity [13, 21]. Moreover, the dissolution of the iron oxide NPs at different conditions should also be considered. For example, at room

temperature (RT), the solubility of ferric oxides with sizes above 11 nm generally follows the reversed order of thermodynamic stability of the crystalline phases, that is, ferrihydrite > lepidocrocite > maghemite > goethite > hematite [22].

This paper reports the peroxidase-like activity of 2-line ferrihydrite (2LFh) and hematite NPs for the degradation of methylene blue (MB) in presence of H_2O_2. The iron oxide NPs selected for this study were two NPs with contrasting properties such as the thermodynamic stability, the size, and the surface area. The catalytic activity of the iron oxide NPs was evaluated by changing the pH conditions, the NPs concentration, and the H_2O_2 concentration. It was demonstrated that the synthesized hematite NPs possess excellent peroxidase-like activity toward the oxidation of MB at high pH. In contrast, due to the metastability of 2LFh, its peroxidase-like activity is suppressed after 15 min and only 69% of MB can be degraded. It is highlighted that the synthetized hematite NPs are cheap and easily prepared from the metastable 2LFh NPs. Hematite NPs exhibited high stability and excellent peroxidase-like activity at basic pH. For these, the hematite NPs are promising materials for the degradation of organic compounds in wastewater treatment plants without the need to decrease the pH of effluents. Therefore, the use of hematite NPs will diminish the process steps for the treatment of wastewater with high content of organic compounds.

2. Experimental Section

2.1. Synthesis of Iron Oxide Nanoparticles. The parent 2LFh NPs were prepared following a modified procedure previously reported [23]. Briefly, 6 mL of a solution of NaOH (6 M) were added into 100 mL of a solution of $FeCl_3$ (0.3 M) and stirred for 5 min. Next, a solution of NaOH (1.0 M) was dropped to the mixture to reach a pH of 8. Once the 2LFh NPs were obtained, the NPs were washed several times with deionized water and dried at RT for 48 h. Otherwise, the hematite NPs were prepared by adding 0.16 g of $FeSO_4{\cdot}7H_2O$ (atomic ratio of Fe(II)/Fe(III) = 0.02) to the freshly prepared parent 2LFh NPs; the mixture was stirred during 10 min; after this, the pH decreased to 6.5. Subsequently, the pH of the solution was adjusted to pH 9.0 with a solution of NaOH (1 M). Finally, 5 mL of a solution of $NaHCO_3$ (1 M) was added, and the reaction was stirred at 95°C for two hours. The product of this reaction was washed with deionized water and dried at RT for 48 h.

2.2. Structural and Morphological Characterization. The crystalline structure of the NPs was obtained by using a Philips diffractometer X'Pert with the Cu(K_α) radiation in the range of 20–80° (2θ). The average crystallite size was obtained by Rietveld refinement of the XRD patterns using the MAUD program version 2.33 [24]. The transmission electron microscopy (TEM) analysis was carried out in a FEI Titan microscope operated at 300 kV. The samples for TEM were prepared by dispersing the NPs in ethanol and dropped on copper grids.

2.3. Measurement of Peroxidase-Like Activity. The catalytic oxidation of MB was evaluated by changing the following parameters: pH (3.6 ± 0.2 and 8 ± 0.2), H_2O_2 concentration (0.075 to 0.6 mol/L), and NPs concentration (1 to 5 g/L). All the catalytic tests were performed in darkness at RT. In a typical experiment, the NPs (2LFh or hematite) were dispersed in 10 mL of MB dissolved in deionized water in a concentration of 10 mg/L; and, in order to start the catalytic degradation, the H_2O_2 solution was added. The MB degradation was monitored by measuring the decrease of its characteristic absorption peak at 665 nm. For this, 2 mL of the suspension was taken off from the reaction media, and in order to separate the NPs from the degraded MB solution, the suspension was centrifuged at 14,000 rpm for 3 min. Next, the absorption spectra of the degraded solutions were measured in a UV-Vis USB 4000 spectrophotometer from Ocean Optics.

Kinetic experiments were done to calculate the reaction rate for different concentration of MB. For this, 0.05 g of 2LFh or hematite NPs were added to 10 mL of an aqueous solution of MB (concentrations from 1 to 20 mg/L) together with H_2O_2 in a concentration of 0.45 mol/L and stirred during 30 min. The pH was maintained at 8 ± 0.2 during the experiments. The kinetic parameters were determined by fitting the absorbance data to the Michaelis–Menten equation [25]:

$$V = V_{\max} \frac{[S]}{[S] + K_m}, \quad (1)$$

where V is the rate of conversion, $V_{\max}$ is the maximal rate of conversion, $[S]$ is the MB concentration, and K_m is the Michaelis constant. K_m is equivalent to the MB concentration for which the rate of conversion is half of $V_{\max}$, and K_m is related to the affinity of the enzyme for the MB.

3. Results and Discussion

3.1. Structural and Morphological Characterization. The crystallinity of the as-prepared 2LFh and hematite NPs was examined by the XRD (see Figure 1). The 2LFh NPs exhibited two broad peaks centered at 35° and 62° (interplanar distances of 0.24 and 0.15 nm), respectively, which are in good agreement with those reported in the literature [23, 26]. The broad diffractions observed in the XRD pattern for 2LFh NPs indicate the presence of a poor crystallized sample. In addition, the XRD pattern of the hematite NPs is in good agreement with the reported one for pure hematite and corresponds to the rhombohedral structure according to the 89-598 JCPDS card. The average crystallite sizes obtained by Rietveld refinement were 5 nm and 100 nm for the 2LFh and hematite NPs, respectively. It is worth mentioning that the XRD results show that the 2LFh NPs were transformed to hematite without the formation of any additional iron oxide polymorph such as goethite, indicating that the synthesis is good enough to produce hematite NPs with high crystallinity.

TEM images show conglomerations of 2LFh NPs with an average size of ~5 nm (see Figure 2(a)). Moreover, Figure 2(b)

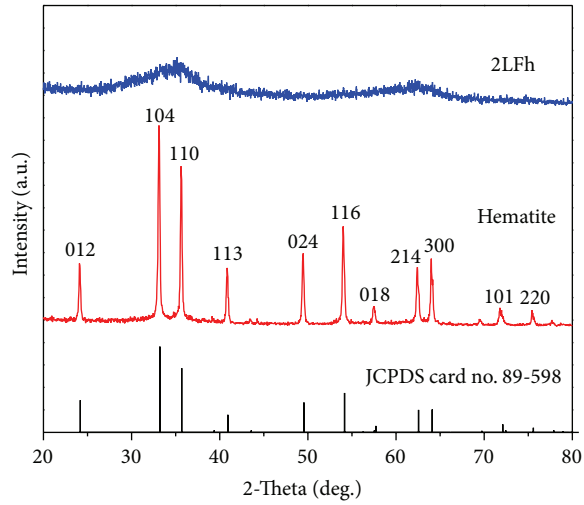

Figure 1: X-Ray diffraction patterns of 2LFh and hematite nanoparticles.

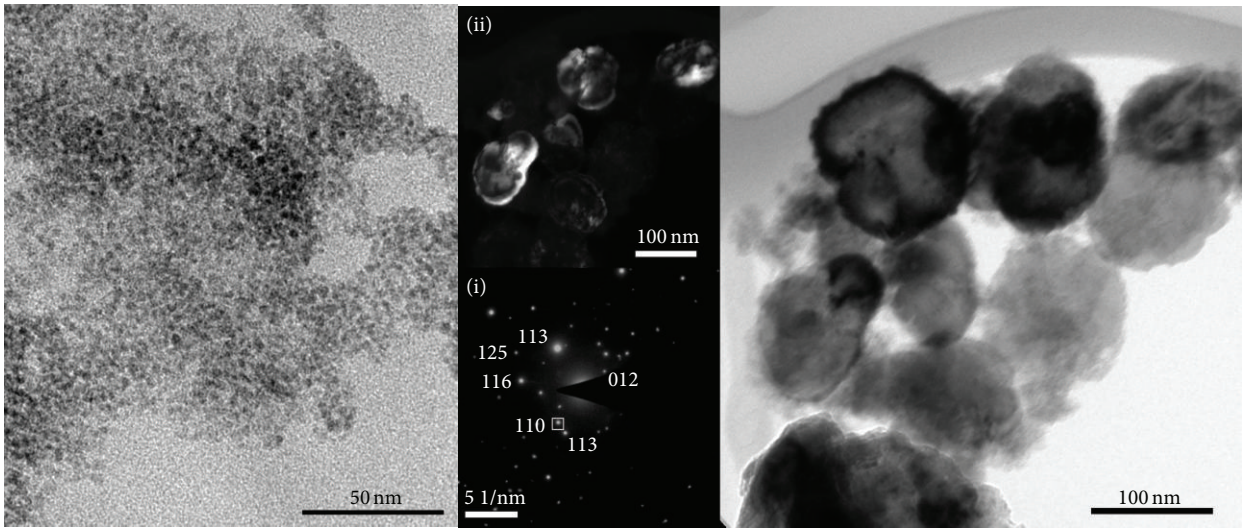

(a) (b)

Figure 2: (a) TEM image of the 2LFh NPs. (b) Typical TEM image of the hematite NPs. The insets: (i) shows the SAED pattern of the aggregate and (ii) shows dark field TEM image obtained with the 110 diffracted beam.

displays the hematite NPs which have an ovoid-like shape with an average size of ~110 nm. Furthermore, the SAED pattern in inset (i) shows the indexation to the (012), (113), (110), (125), and (116) crystalline planes of the hematite structure. Inset (ii) shows a dark field TEM image obtained with the 110 diffracted beam; some very bright hematite NPs denote strongly diffracting single crystals; however, some darker areas are seen on the nanoparticles. It indicates a strong agglomeration of particles of different sizes.

3.2. Peroxidase-Like Activity. The peroxidase-like activity of the as-prepared 2LFh and hematite NPs was evaluated by measuring the degradation percentage of the MB with and without H_2O_2. The catalytic activity of the NPs was estimated by using the following equation:

$$\text{Degradation (\%)} = \frac{I_t - I_0}{I_0} \times 100, \quad (2)$$

where I_0 is the absorbance intensity of the MB solution at the beginning of the experiments (without iron oxide NPs) and I_t is the absorbance intensity after mixing the iron oxide NPs with the solution of MB at a specific time (t). Hence, a decrement in I_t indicates that there is a degradation of MB in the aqueous solution [27].

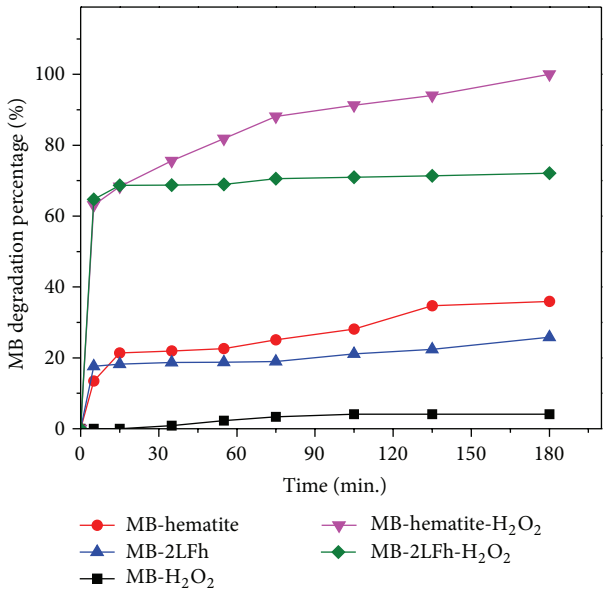

FIGURE 3: Peroxidase-like activity of 2LFh and hematite NPs using different systems. Reaction conditions: pH 8, 5 g/L of NPs, 0.45 mol/L of H_2O_2, and 10 mg/L of MB.

As observed in Figure 3, the MB degradation percentage was only 3% after 180 min if only H_2O_2 was employed for the MB degradation; this points out that the oxidation of MB with solely H_2O_2 is very limited. When the 2LFh or hematite NPs were added into the MB solution (without H_2O_2), the MB degradation percentage increased up to 30% and 40%, respectively. This decrease of MB concentration was caused probably by the adsorption of MB on the surface of the NPs and/or due to the oxidation of MB induced by residual dissolved oxygen [28]. Otherwise, when hematite or 2LFh NPs were added into the MB solution in presence of H_2O_2, the hematite NPs were able to completely degrade the MB dye after 180 min of reaction, while the 2LFh NPs oxidized only 72% (see Figure 3). This indicates that the interactions among the NPs and H_2O_2 are essential for the catalytic degradation of MB.

The results suggest that the NPs diminish the concentration of MB mostly by the MB decomposition rather than by its adsorption. It has been proposed that hydroxyl radicals (•OHs) are formed by the H_2O_2 decomposition, which is induced by the presence of iron oxide NPs [13]. In consequence, the MB molecules adsorbed on the surface of the NPs are oxidized by hydroxyl radicals generated by the peroxidase-like catalytic activity of the NPs; this process is named Fenton-like oxidation [13]. A possible reaction mechanism for this type of reactions can be as follows: First, the MB molecules are adsorbed on iron oxide NPs. Next, the H_2O_2 added to the MB solution in the presence of iron oxide NPs is also adsorbed on the surface of the NPs. Consequently, the adsorbed H_2O_2 reacts with the active sites of the iron oxide NPs to produce Fe(III)-H_2O_2 superficial species; then, the absorbed H_2O_2 reacts with the superficial sites generating highly reactive free radicals such as •OH and Fe(II) superficial species [13, 29]. Finally, the MB molecules adsorbed on the NPs are oxidized by the •OH free radicals.

In order to characterize the peroxidase-like activity of 2LFh and hematite NPs, the degradation of MB was monitored by observing the decrease of the absorbance peak at 664 nm of MB at different reaction times. As depicted in Figure 4, the absorbance decreased drastically after 5 min when both 2LFh and hematite NPs were utilized in presence of H_2O_2. After this time, the hematite NPs continue degrading the MB to reach a total degradation of ~100% after 180 min. However, the 2LFh NPs cannot degrade more MB after 5 min of reaction, since there is no change in the absorbance intensity after this time (see Figure 4(a)). This result suggests that the catalytic activity of the poorly crystallized 2LFh NPs is limited to only short periods of time. In contrast, the highly crystalline hematite NPs were able to degrade completely the MB solution after 180 min of reaction. Thus, the peroxidase-like activity depends on the crystalline structure of the NPs; this behavior has also been reported for magnetite, hematite, and goethite [30].

3.3. Influence of pH. Since the stability of iron oxide NPs depends on the pH, the degradation experiments were realized at different pH values in presence of H_2O_2. As observed in Figure 5(a), at pH 3.6, the MB degradation was 24% and 33% for the hematite and 2LFh NPs, respectively. The degradation percentage was higher for 2LFh than for hematite NPs; it is because the 2LFh NPs are dissolved at pH of 3.6 [13]. The dissolution of 2LFh forms aqueous Fe^{3+} ions which promote the degradation of MB through the classic Fenton reaction [31]. The higher degradation of MB observed with 2LFh NPs at pH 3.6 is in agreement with other results, where the ferrihydrite dissolution was reported, which assists the degradation of atrazine in presence of H_2O_2 at pH between 3 and 4 [31].

At higher pH, after 180 min of reaction, 72% and 100% of MB degradation were reached for 2LFh and hematite NPs, respectively. This result suggests that the NPs generated higher levels of •OH radicals at pH = 8 than at pH = 3.6. Additionally, the iron oxide NPs are not dissolved at basic pH; this, in turn, allows the production of more •OH radicals which helps to degrade greater amounts of MB. It is worth mentioning that the degradation percentage of MB was almost constant (around 68–72%) for the 2LFh NPs after a time of 30 min; this means that the degradation properties of these NPs are deactivated after 30 min of reaction (see Figure 5(a)). The high catalytic activity for hematite at pH 8 is consistent with previous reports [32], which indicated that hematite NPs induced higher levels of •OH radicals than γ-Fe_2O_3 (maghemite) NPs at neutral pH. In addition, our findings agree with other results, where the decomposition percentage of H_2O_2 was three times higher at pH 8 than at pH 3 [31].

According to the literature, wastewater treatment of organic substances through the typical Fenton reaction is efficient at pH 3–3.6, where the •OH species are generated [33]. However, wastewater from industries may have higher pH values, laying in the range of 6.5 to 8.5, where it is

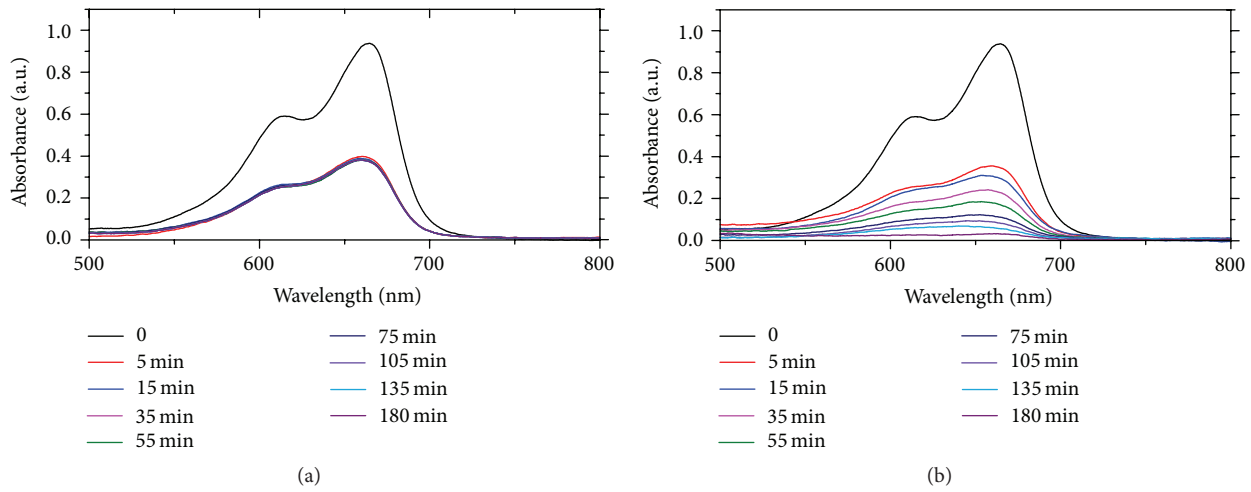

FIGURE 4: The time-dependent absorbance spectra of the degraded MB solution using (a) 2LFh and (b) hematite NPs catalysts. Reaction conditions: pH 8, 5 g/L of NPs, 0.45 mol/L of H_2O_2, and 10 mg/L of MB.

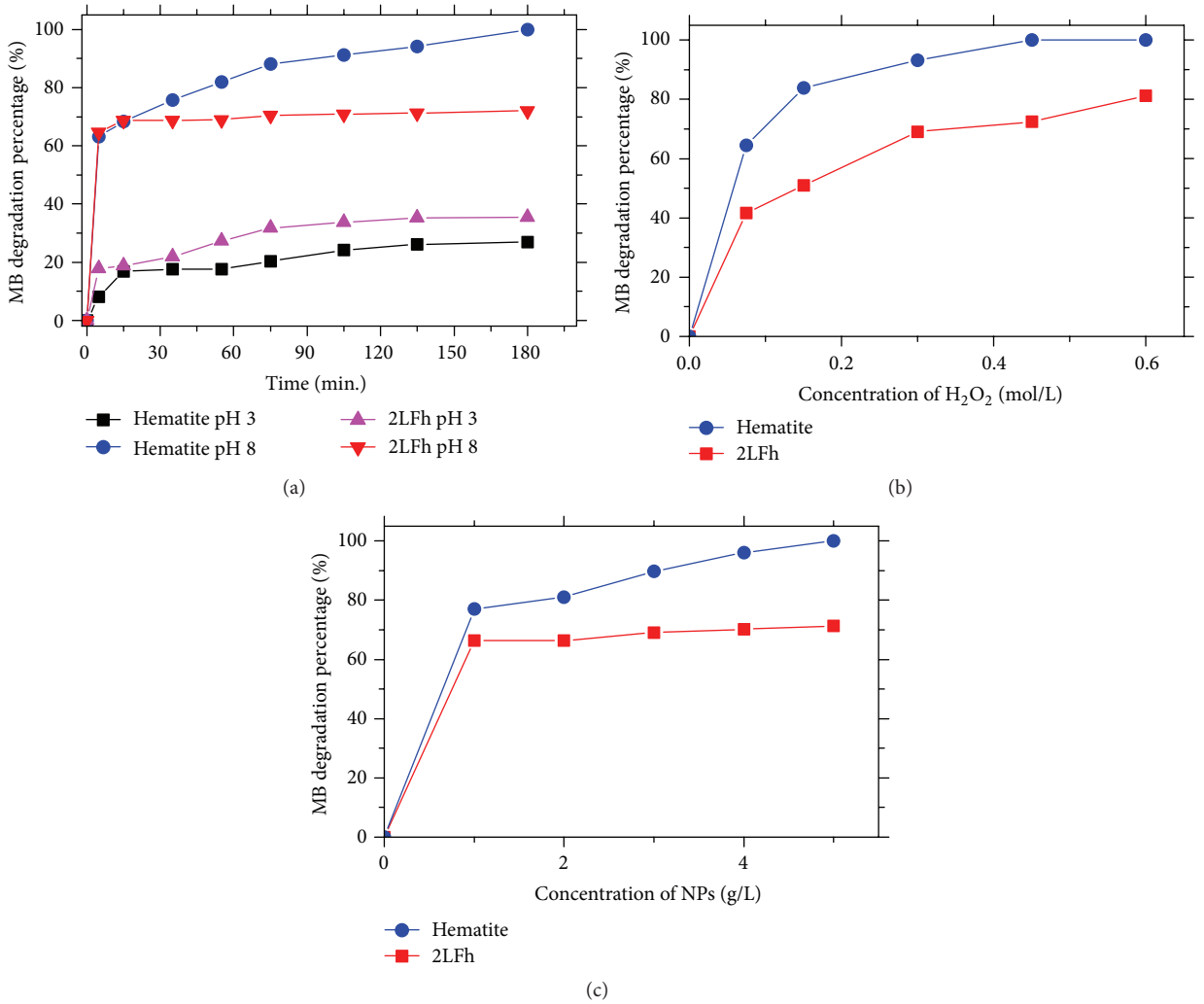

FIGURE 5: Curves of MB degradation as a function of (a) reaction time (0.45 mol/L of H_2O_2, 0.5 g/L of NPs, and 10 mg/mL of MB), (b) H_2O_2 concentration (time 180 min, pH 8, 0.5 g/L of NPs, and 10 mg/mL of MB), and (c) concentration of NPs (time 180 min, 0.45 mol/L of H_2O_2, and pH 8, 10 mg/mL of MB).

compulsory to decrease the pH for degradation of organic pollutants through the Fenton reaction [34]. Our results indicate that iron oxide NPs can be useful to oxidize organic pollutants in greater extent at basic conditions these finding are suitable for the degradation of organic compounds from basic wastewaters without decreasing the pH.

3.4. Influence of H_2O_2 Concentration. Figure 5(b) shows the MB degradation percentage as a function of the H_2O_2 concentration. By rising the H_2O_2 concentration, the degradation percentage of MB increases as well. This result is congruent with previous publications [31, 35]. The concentration of H_2O_2 is directly related to the amount of hydroxyl radicals produced in the catalytic reaction, which, in turn, rises the degradation percentage of MB [36]. Moreover, in the case of hematite NPs, the total degradation of MB was observed for an H_2O_2concentration of 0.45 mol/L (see Figure 5(b)). Thus, an excess of H_2O_2 in the solution implies a decrease in the production rate of •OH radicals. If high concentrations of H_2O_2 are used, most of the H_2O_2 will not have MB molecules to degrade; in consequence, many free radicals might be wasted. Additionally, an excess of H_2O_2 also inhibits the formation of •OH free radicals and produces hydroperoxide radicals which do not contribute to the MB oxidation [11, 37, 38].

In the case of 2LFh NPs, a total degradation of MB was not reached even though a concentration as high as 0.6 mol/L of H_2O_2 was employed; only 79% of MB was degraded (see Figure 5(b)). Surely, the 2LFh NPs had a lower catalytic degradation activity than hematite NPs; it is because there were lower number of active superficial sites available for both the adsorption of H_2O_2 and the formation of •OH free radicals. This result is in agreement with other works that used a comparative study with other iron oxides, where higher production of •OH radicals was reported by hematite NPs [32]. Through these experiments, the best conditions for obtaining the highest MB degradation percentage were found, which are a pH of 8 and an H_2O_2 concentration of 0.45 mol/L. These conditions were used for the Michaelis–Menten kinetics experiments.

3.5. Influence of NPs Concentration. The MB degradation percentage augmented by increasing the NPs concentration (for both 2LFh and hematite) within the range of 0 to 5 g/L as shown in Figure 5(c). The total degradation of MB was observed when a concentration of 5 g/L of hematite was employed; on the other hand, there were not changes in the degradation percentage for concentrations higher than 3 g/L of 2LFh NPs (see Figure 5(c)). According to the literature, the formation rate of •OH should be proportional to the available active superficial sites; it means that larger surface area should produce a higher catalytic activity [29, 36, 39]. Thus, it would be reasonable to expect that the 2LFh NPs with a size of ~5 nm would have higher catalytic activity than hematite NPs (size ~110 nm). However, the MB degradation percentage was lower for 2LFh NPs than for hematite NPs (see Figure 5(c)). This discrepancy may be due to the fact that 2LFh tends to agglomerate in aqueous media; it is because the size of the agglomerates increases at higher NPs concentration [29]. Therefore, the active superficial sites of 2LFh NPs could be reduced due to the formation of big agglomerates [29, 40]. Consequently, there are fewer active superficial sites available for the adsorption of H_2O_2 molecules, which limits its decomposition. Hence, the agglomeration of 2LFh NPs could contribute to their lower performance for the MB degradation.

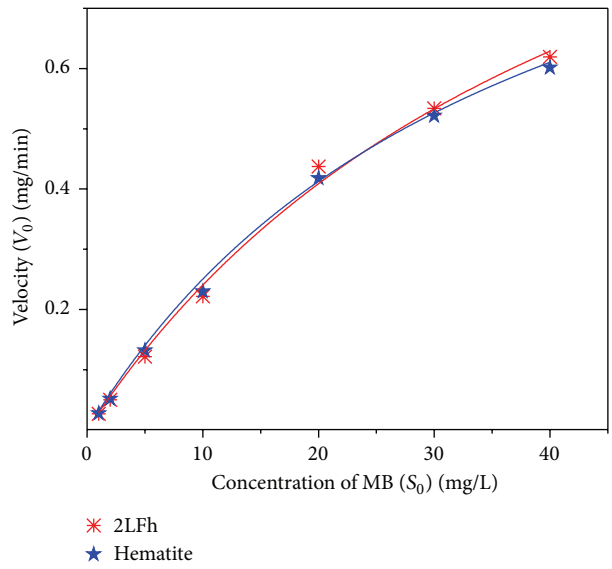

Figure 6: Steady-state kinetic assay of 2LFh and hematite NPs. Reaction conditions: pH 8, RT, 5 g/L of NPs, 0.45 mol/L of H_2O_2, and 10 mg/L of MB.

3.6. Michaelis–Menten Kinetic Analysis. The Michaelis–Menten kinetics describes an enzymatic reaction, which is based on the assumption that the enzyme-substrate complex maintains a steady state; that is, its concentration does not change [41]. Figure 6 shows the Michaelis–Menten kinetic analysis for the degradation of MB by varying the MB concentration. To obtain the kinetic parameters (V_{max} and K_m), the data were fitted to the Michaelis–Menten equation. Additionally, the catalytic constant K_{cat} was calculated according to [41]

$$K_{cat} = \frac{V_{max}}{[E]}, \tag{3}$$

where $[E]$ was taken as the NPs concentration. K_m is an indicator of affinity between the enzymes and the organic compound to be degraded. In this case, it is a measure of the affinity between the iron oxide NPs and the MB molecules. A high K_m represents a weak affinity for the substrate, whereas a low value suggests a high affinity [25]. The parameter K_{cat} is considered a measure of the maximum catalytic degradation under saturating dye conditions per unit of time per unit of enzyme, while V_{max} is the maximum rate of reaction. As the value of K_{cat} increases, the catalytic activity is faster [25].

Table 1: Michaelis–Menten parameters of the tested nanoparticles.

NPs	K_m (mg/L)	V_{max} (mg/min)	K_{cat} (1/min)
Hematite	36.82	1.36	0.273
2LFh	46.67	1.17	0.234

As observed in Table 1, K_m was lower for the hematite NPs, which indicates that hematite has higher affinity for MB than 2LFh. Additionally, V_{max} and K_{cat} were higher for hematite NPs; this indicates that the catalytic activity for hematite is higher than that for 2LFh NPs. Therefore, hematite NPs exhibit higher peroxide-like activity than 2LFh.

The evaluation of the peroxidase-like activity of the product of the transformation of 2LFh has not been reported in the literature. However, it has been shown that crystalline α-Fe_2O_3 NPs exhibited higher catalytic efficiency for the decomposition of hydrogen peroxide than amorphous Fe_2O_3 NPs [20]. Usually, the rate of a catalytic process is a function of surface area, which increases rapidly with decreasing particle size [22]. In contrast, a more complex role of the "surface quality" of the catalysts has been reported in different catalytic processes [20]. In this sense, the ordered surface of the hematite NPs has a stronger effect for the degradation of MB than its low surface area. The same results were achieved in the degradation of H_2O_2 mediated iron oxides with different crystallization degree, concluding that the crystal planes of the catalysts affect the catalytic process more significantly than the high surface area of the oxides [20].

4. Conclusions

Both 2LFh and hematite NPs presented peroxidase-like activity for the degradation of MB in presence of H_2O_2. At pH 8, the degradation percentage of MB was 100% and 69% for hematite and 2LFh NPs, respectively. The reduced and suppressed catalytic activity of 2LFh NPs was associated with its poor crystallinity and its metastability, as well as its strong agglomeration in aqueous media. The pH was an important factor for the catalytic degradation, since a maximum degradation of 24% was obtained at a pH of 3.6, while at pH of 8, up to 100% of MB degradation was obtained. According to the optimization experiments, the best conditions for degradation of MB using hematite NPs were pH 8, H_2O_2 concentration of 0.45 mol/L, and NPs concentration of 5 g/L. According to the kinetic analysis, the V_{max} and K_{cat} parameters were higher for hematite NPs, indicating that their catalytic activity was higher than that for 2LFh NPs. It has been concluded that the ordered surface of the hematite NPs has a stronger effect for the degradation of MB than its surface area. Thus, it has been demonstrated that hematite NPs could be a promising catalyst for degradation of organic compounds in wastewaters with high pH.

Competing Interests

The authors declare that they have no competing interests.

Acknowledgments

This work was supported by the Multidisciplinary Projects Initiative of Cinvestav. The authors appreciate the assistance of Alvaro Angeles Pascual for the TEM measurements.

References

[1] G. Battistuzzi, M. Bellei, C. A. Bortolotti, and M. Sola, "Redox properties of heme peroxidases," *Archives of Biochemistry and Biophysics*, vol. 500, no. 1, pp. 21–36, 2010.

[2] H. Wei and E. Wang, "Nanomaterials with enzyme-like characteristics (nanozymes): next-generation artificial enzymes," *Chemical Society Reviews*, vol. 42, no. 14, pp. 6060–6093, 2013.

[3] P. Sharma, A. B. Jha, R. S. Dubey, and M. Pessarakli, "Reactive oxygen species, oxidative damage, and antioxidative defense mechanism in plants under stressful conditions," *Journal of Botany*, vol. 2012, Article ID 217037, 26 pages, 2012.

[4] M. Hamid and Khalil-ur-Rehman, "Potential applications of peroxidases," *Food Chemistry*, vol. 115, no. 4, pp. 1177–1186, 2009.

[5] R. Andreozzi, V. Caprio, A. Insola, and R. Marotta, "Advanced oxidation processes (AOP) for water purification and recovery," *Catalysis Today*, vol. 53, no. 1, pp. 51–59, 1999.

[6] V. A. Cooper and J. A. Nicell, "Removal of phenols from a foundry wastewater using horseradish peroxidase," *Water Research*, vol. 30, no. 4, pp. 954–964, 1996.

[7] E. S. Henle, Y. Luo, and S. Linn, "Fe^{2+}, Fe^{3+}, and oxygen react with DNA-derived radicals formed during iron-mediated Fenton reactions," *Biochemistry*, vol. 35, no. 37, pp. 12212–12219, 1996.

[8] N. Durán and E. Esposito, "Potential applications of oxidative enzymes and phenoloxidase-like compounds in wastewater and soil treatment: a review," *Applied Catalysis B: Environmental*, vol. 28, no. 2, pp. 83–99, 2000.

[9] R. André, F. Natálio, and W. Tremel, "Nanoparticles as enzyme mimics," in *New and Future Developments in Catalysis*, S. Suib, Ed., Nanoparticles, pp. 149–173, Elsevier, 2013.

[10] L. Zhou, Y. Shao, J. Liu et al., "Preparation and characterization of magnetic porous carbon microspheres for removal of methylene blue by a heterogeneous fenton reaction," *ACS Applied Materials and Interfaces*, vol. 6, no. 10, pp. 7275–7285, 2014.

[11] N. Wang, L. Zhu, M. Wang, D. Wang, and H. Tang, "Sono-enhanced degradation of dye pollutants with the use of H_2O_2 activated by Fe_3O_4 magnetic nanoparticles as peroxidase mimetic," *Ultrasonics Sonochemistry*, vol. 17, no. 1, pp. 78–83, 2010.

[12] L. Gao, J. Zhuang, L. Nie et al., "Intrinsic peroxidase-like activity of ferromagnetic nanoparticles," *Nature Nanotechnology*, vol. 2, no. 9, pp. 577–583, 2007.

[13] W. P. Kwan and B. M. Voelker, "Rates of hydroxyl radical generation and organic compound oxidation in mineral-catalyzed fenton-like systems," *Environmental Science and Technology*, vol. 37, no. 6, pp. 1150–1158, 2003.

[14] F. Yu, Y. Huang, A. J. Cole, and V. C. Yang, "The artificial peroxidase activity of magnetic iron oxide nanoparticles and its application to glucose detection," *Biomaterials*, vol. 30, no. 27, pp. 4716–4722, 2009.

[15] N. Wang, L. Zhu, D. Wang, M. Wang, Z. Lin, and H. Tang, "Sono-assisted preparation of highly-efficient peroxidase-like Fe_3O_4 magnetic nanoparticles for catalytic removal of organic pollutants with H_2O_2," *Ultrasonics Sonochemistry*, vol. 17, no. 3, pp. 526–533, 2010.

[16] X.-Q. Zhang, S.-W. Gong, Y. Zhang, T. Yang, C.-Y. Wang, and N. Gu, "Prussian blue modified iron oxide magnetic nanoparticles and their high peroxidase-like activity," *Journal of Materials Chemistry*, vol. 20, no. 24, pp. 5110–5116, 2010.

[17] S. Belattar, Y. Mameri, N. Seraghni, N. Debbache, and T. Sehili, "Catalytic degradation of 3,5-dimethylphenol with goethite and hydrogen peroxide," *Journal of Environmental Engineering and Technology*, vol. 1, no. 3, pp. 21–28, 2012.

[18] K. N. Chaudhari, N. K. Chaudhari, and J.-S. Yu, "Peroxidase mimic activity of hematite iron oxides (α-Fe_2O_3) with different nanostructures," *Catalysis Science and Technology*, vol. 2, no. 1, pp. 119–124, 2012.

[19] W. Chen, J. Chen, A.-L. Liu, L.-M. Wang, G.-W. Li, and X.-H. Lin, "Peroxidase-like activity of cupric oxide nanoparticle," *ChemCatChem*, vol. 3, no. 7, pp. 1151–1154, 2011.

[20] M. Hermanek, R. Zboril, I. Medrik, J. Pechousek, and C. Gregor, "Catalytic efficiency of iron(III) oxides in decomposition of hydrogen peroxide: competition between the surface area and crystallinity of nanoparticles," *Journal of the American Chemical Society*, vol. 129, no. 35, pp. 10929–10936, 2007.

[21] R. Matta, K. Hanna, and S. Chiron, "Fenton-like oxidation of 2,4,6-trinitrotoluene using different iron minerals," *Science of the Total Environment*, vol. 385, no. 1–3, pp. 242–251, 2007.

[22] H. Wu, J.-J. Yin, W. G. Wamer, M. Zeng, and Y. M. Lo, "Reactive oxygen species-related activities of nano-iron metal and nano-iron oxides," *Journal of Food and Drug Analysis*, vol. 22, no. 1, pp. 86–94, 2014.

[23] U. Schwertmann and R. M. Cornell, *Iron Oxides in Laboratory: Preparation and Characterization*, John Wiley & Sons, Weinheim, Germany, 2nd edition, 2000.

[24] L. Lutterotti, M. Bortolotti, G. Ischia, I. Lonardelli, and H.-R. Wenk, "Rietveld texture analysis from diffraction images," *Zeitschrift für Kristallographie Supplements*, vol. 2007, supplement 26, pp. 125–130, 2007.

[25] A. Rogers and Y. Gibon, "Enzyme kinetics: theory and practice," in *Plant Metabolic Networks*, J. Schwender, Ed., pp. 71–103, Springer, New York, NY, USA, 2009.

[26] H. Liu, P. Li, B. Lu, Y. Wei, and Y. Sun, "Transformation of ferrihydrite in the presence or absence of trace Fe(II): the effect of preparation procedures of ferrihydrite," *Journal of Solid State Chemistry*, vol. 182, no. 7, pp. 1767–1771, 2009.

[27] C. R. García, J. Oliva, and L. A. Díaz-Torres, "Photocatalytic activity of $LaSr_2AlO_5$:Eu ceramic powders," *Photochemistry and Photobiology*, vol. 91, no. 3, pp. 505–509, 2015.

[28] Q. Chang, K. Deng, L. Zhu, G. Jiang, C. Yu, and H. Tang, "Determination of hydrogen peroxide with the aid of peroxidase-like Fe_3O_4 magnetic nanoparticles as the catalyst," *Microchimica Acta*, vol. 165, no. 3-4, pp. 299–305, 2009.

[29] K. Rusevova, F.-D. Kopinke, and A. Georgi, "Nano-sized magnetic iron oxides as catalysts for heterogeneous Fenton-like reactions-influence of Fe(II)/Fe(III) ratio on catalytic performance," *Journal of Hazardous Materials*, vol. 241-242, pp. 433–440, 2012.

[30] S. Lee, J. Oh, and Y. Park, "Degradation of phenol with fenton-like treatment by using heterogeneous catalyst (modified iron oxide) and hydrogen peroxide," *Bulletin of the Korean Chemical Society*, vol. 27, no. 4, pp. 489–494, 2006.

[31] J. C. Barreiro, M. D. Capelato, L. Martin-Neto, and H. C. Bruun Hansen, "Oxidative decomposition of atrazine by a Fenton-like reaction in a H_2O_2/ferrihydrite system," *Water Research*, vol. 41, no. 1, pp. 55–62, 2007.

[32] B. Wang, J.-J. Yin, X. Zhou et al., "Physicochemical origin for free radical generation of iron oxide nanoparticles in biomicroenvironment: catalytic activities mediated by surface chemical states," *The Journal of Physical Chemistry C*, vol. 117, no. 1, pp. 383–392, 2013.

[33] E. Neyens and J. Baeyens, "A review of classic Fenton's peroxidation as an advanced oxidation technique," *Journal of Hazardous Materials*, vol. 98, no. 1–3, pp. 33–50, 2003.

[34] Z. Carmen and S. Daniela, "Textile organic dyes—characteristics, polluting effects and separation/elimination procedures from industrial effluents—a critical overview," in *Organic Pollutants Ten Years after the Stockholm Convention—Environmental and Analytical*, T. Puzyn, Ed., p. 472, InTech, 2010.

[35] L. Gao, K. M. Giglio, J. L. Nelson, H. Sondermann, and A. J. Travis, "Ferromagnetic nanoparticles with peroxidase-like activity enhance the cleavage of biological macromolecules for biofilm elimination," *Nanoscale*, vol. 6, no. 5, pp. 2588–2593, 2014.

[36] E. G. Garrido-Ramírez, B. K. G. Theng, and M. L. Mora, "Clays and oxide minerals as catalysts and nanocatalysts in Fenton-like reactions—a review," *Applied Clay Science*, vol. 47, no. 3-4, pp. 182–192, 2010.

[37] J. J. Wu, M. Muruganandham, J. S. Yang, and S. S. Lin, "Oxidation of DMSO on goethite catalyst in the presence of H_2O_2 at neutral pH," *Catalysis Communications*, vol. 7, no. 11, pp. 901–906, 2006.

[38] H. Lee, S. Do, and S. Kong, "The role of Magnetite Nano Particle (MNP) to oxidize nitrobenzene using heterogeneous fenton reaction in," in *Proceedings of the World Congress on Engineering and Computer Science*, pp. 20–23, San Francisco, Calif, USA, 2010.

[39] I. S. X. Pinto, P. H. V. V. Pacheco, J. V. Coelho et al., "Nanostructured δ-FeOOH: an efficient fenton-like catalyst for the oxidation of organics in water," *Applied Catalysis B: Environmental*, vol. 119-120, pp. 175–182, 2012.

[40] X. Xue, K. Hanna, and N. Deng, "Fenton-like oxidation of Rhodamine B in the presence of two types of iron (II, III) oxide," *Journal of Hazardous Materials*, vol. 166, no. 1, pp. 407–414, 2009.

[41] J. G. Voet and D. Voet, "Rates of enzymatic reactions," in *Biochemistry*, pp. 482–505, 2011.